EPJ Web of Conferences **86**, 00044 (2015)
DOI: 10.1051/epjconf/ 20158600044

Fusion excitation function measurement for ^{6}Li+^{64}Ni at near-barrier energies

Md. Moin Shaikh[1,a], Subinit Roy[1], S. Rajbanshi[1], M. K. Pradhan[1], A. Mukherjee[1], P. Basu[1], S. Pal[2], V. Nanal[2], R. G. Pillay[2], and A. Shrivastava[3]

[1] *Saha Institute of Nuclear Physics, 1/AF, Bidhan Nagar, Kolkata-700 064, INDIA*
[2] *Department of Nuclear and Atomic Physics, Tata Institute of Fundamental Research, Mumbai-400 005, INDIA*
[3] *Nuclear Physics Division, Bhabha Atomic Research Centre, Mumbai-400 085, INDIA*

Abstract. Total fusion excitation function has been measured for the reaction of weakly bound ^{6}Li projectile on medium mass ^{64}Ni target at energies near the Coulomb barrier of the system. Online characteristic γ-ray detection method has been used to identify and determine the cross sections of the residues. No suppression of total fusion cross section (σ_{TF}) is observed at above barrier energies. But enhancement of measured cross section with respect to the one-dimensional barrier penetration model (1-DBPM) calculation is observed at below barrier energies. The enhancement can not be explained by coupled channels calculation with dominant projectile and target excitations as well as one-neutron stripping reaction.

1 Introduction

Reactions with weakly bound stable projectiles have been studied on several targets [1–6] in order to investigate the role of breakup channel on fusion in different mass regions. The complete fusion (CF) cross sections in reactions with weakly bound nuclei at energies above the barrier is said to be suppressed compared to the prediction of one-dimensional barrier penetration model (1-DBPM). The suppression of complete fusion (CF) is accounted for with the process of incomplete fusion (ICF) of a part of the weakly bound projectile with the target. Experimentally, the suppression effect is distinctly observed for heavy targets [1]. It is argued that the suppression will decrease with the decrease of charge product of the colliding system [7–9] indicating the role of Coulomb interaction in the process. An altogether diffrent observation also exists in the literature [10], that predicted a uniform suppression of complete fusion cross section for ^{6}Li induced fusion and attributed the effect to the dominance of nuclear induced breakup over Coulomb breakup for ^{6}Li. However, the verification of the conjectures depend solely on the separation of CF process from ICF process. While the experimental separation of CF and ICF is possible for heavy targets, it is difficult for medium or light mass targets. In reactions with light and medium mass targets, the weakly bound projectiles populate same residues from CF and ICF processes. So, the total fusion (TF = CF+ICF) is measured and compared with model prediction. The questions that arise for these targets are - how does breakup affect the total fusion cross section and whether it is enhanced or suppressed at below the barrier energies? In this context, we present here our recent measurement of fusion excitation function for weakly bound projectile ^{6}Li (S_{α}= 1.47 MeV) with medium mass target ^{64}Ni at near-barrier energies. The elastic scattering measurement for this system [11] indicates the presence of breakup threshold anomaly (BTA) or breakup induced threshold behaviour of effective interaction potential around the barrier. Hence, it will be interesting to see the effect of breakup or breakup like processes on fusion at these energies.

2 Setup and Experimental Details

The experiment was carried out at BARC-TIFR Pelletron Facility in Mumbai, India. A self-supporting ~99% enriched metallic ^{64}Ni target of thickness 507 μg/cm^2, procured from Oak Ridge National Laboratory, USA, had been used for the present experiment. The target thickness was verified with the α-energy loss method using a 3-line α source (^{239}Pu, ^{241}Am and ^{244}Cm) and estimated uncertainty was about 2%. The target was bombarded with ^{6}Li beam obtained from the Pelletron at energies from 11 to 28 MeV in small steps. The background spectra were recorded without the beam and also with the beam through a blank Tantalum frame in place of the target at the end of each energy run. The fusion cross sections were measured by detecting the prompt characteristic γ-rays emitted by the evaporation residues using the method as described in Ref. [12]. An n-type HPGe detector and another p-type HPGe detector were placed at 45° and 125° respectively with respect to the beam direction to detect the γ-rays. The detectors resolutions were 2.8 and 2.3 keV respectively for 1408 keV γ-line of ^{152}Eu radioactive source. The calibration and the absolute efficiency run were taken by placing calibrated standard radioactive sources ^{152}Eu and ^{133}Ba at the position of the target before and after the ex-

[a] e-mail: moin.shaikh@saha.ac.in

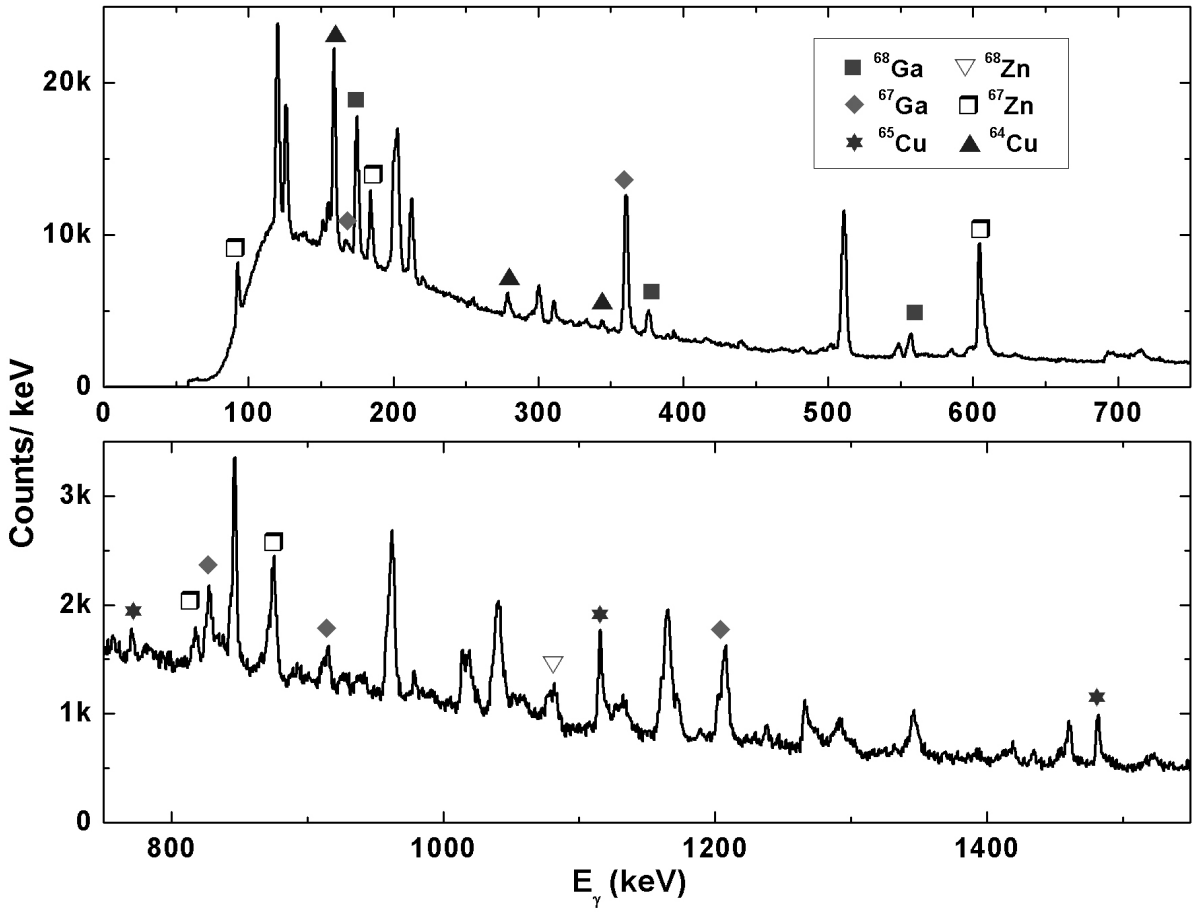

Figure 1. Representative characteristic γ-spectrum from ^{6}Li+^{64}Ni fusion at E_{lab}= 26 MeV.

periment. The data were recorded using the data acquisition system LAMPS [13]. The number of beam particles was estimated from the beam current measured with the help of an 1 m long insulated Faraday cup. The total uncertainty in the measurement of cross sections came from the systematic uncertainties in the target thickness as well as the measurement of the beam particles and the statistical error in determining the yields of γ-rays. A representative γ-ray spectrum recorded at E_{lab} = 26 MeV is shown in Fig. 1. Some of the observed γ-lines are marked on the spectrum.

3 Analysis and Results

In the fusion of ^{6}Li+^{64}Ni the compound nucleus formed is ^{70}Ga. The most dominating decay channels are 2n and 3n evaporation channels. The pn, $p2n$ or dn, αn and α2n decay channels are also observed. The residues produced from the $p2n$/dn, αn and α2n channels can also be produced via the ICF process through the fusion of one of the cluster components (α or d) with the target nucleus ^{64}Ni. Cross section of each residue has been obtained by summing measured cross sections of the prompt characteristic γ-rays form the transitions to the ground state of that residue. The observed γ-ray transitions to the ground state of each residue are given in the Table 1. One of the limitation of the characteristic γ-ray detection method is that the contribution of direct ground state deacy of the excited compound nucleus can not be obtained from this measurement. However it had been shown that the direct ground state feeding is negligibly small for this target mass region [12, 14, 15]. The residues populated in the ICF process could not be distinguished experimentally from those produced in the CF process. In Fig. 2, a comparison of the summed experimental cross sections of 2n and 3n channels with the statistical model prediction from PACE4 [16] has been shown. As these two channels are populated primarily from pure CF decay, statistical model decribes the data quite nicely. On the other hand, the model fails to reproduce the measured excitation function for the αn decay channel producing the residue ^{65}Cu. The residue can also be produced by d-ICF and/or transfer processes. It is to be noted that the αn channel has even larger cross section than the summed 2n and 3n channel at lower energies below the barrier. This clearly indicates the presence non-compound nuclear reaction processes. The total fusion cross sections (σ_{TF}) were obtained by summing the cross sections of all the evaporation residues. The total fusion excitation function has been shown in the Fig. 3 with solid bullets. The fusion excitation function predicted by 1-DBPM calculation is shown by the dashed line in the Fig. 3. The Aky*üz*-Winther potential [17] in Woods-Saxon

Table 1. Observed γ-ray transitions to the ground states

Residues Channel	Transitions (Ex. state→g.s.)	E_γ (keV)
^{68}Ga (2n)	$2^+ \rightarrow 1^+$	175.0
	$1^+ \rightarrow 1^+$	321.0
	$3^+ \rightarrow 1^+$	374.6
	$3^+ \rightarrow 1^+$	555.5
	$2^+ \rightarrow 1^+$	564.5
	$2^- \rightarrow 1^+$	584.0
^{67}Ga (3n)	$1/2^- \rightarrow 3/2^-$	167.0
	$5/2^- \rightarrow 3/2^-$	359.1
	$3/2^- \rightarrow 3/2^-$	828.1
	$5/2^- \rightarrow 3/2^-$	910.9
	$7/2^- \rightarrow 3/2^-$	1202.3
^{68}Zn(pn)	$2^+ \rightarrow 0^+$	1077.4
^{67}Zn (p2n/dn)	$3/2^- \rightarrow 5/2^-$	184.6
	$3/2^- \rightarrow 5/2^-$	393.5
	$9/2^+ \rightarrow 5/2^-$	604.5
	$7/2^- \rightarrow 5/2^-$	814.8
	$3/2^- \rightarrow 5/2^-$	870.9
	$5/2^+ \rightarrow 5/2^-$	979.9
^{65}Cu (αn)	$1/2^- \rightarrow 3/2^-$	770.6
	$5/2^- \rightarrow 3/2^-$	1156.6
	$7/2^- \rightarrow 3/2^-$	1482.0
^{64}Cu (α2n)	$2^+ \rightarrow 0^+$	159.3
	$2^+ \rightarrow 0^+$	278.2
	$1^+ \rightarrow 0^+$	344.0

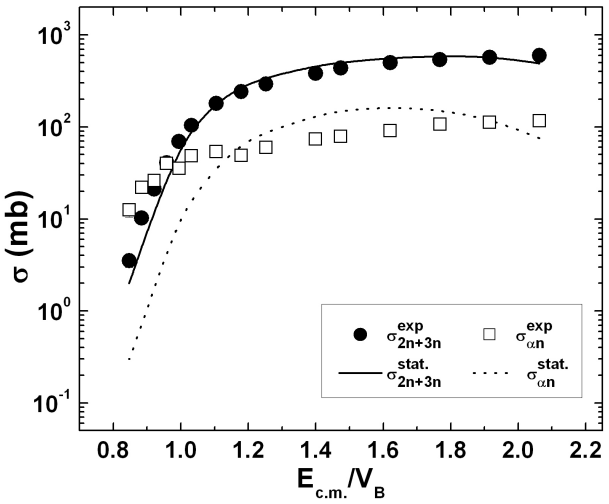

Figure 2. Experimental excitation functions of summed cross sections of $2n$ and $3n$ channels and the cross section of αn channel are shown in comparison with the statistical model predictions.

form is used in the calculation. The used potential parameter values were: strength V_0 = 41.47 MeV, radius parameter r_0 = 1.17 fm and diffuseness a_0 = 0.60 fm. The resultant uncoupled barrier height V_B, barrier radius R_B and the curvature $\hbar\omega$ obtained yielded by the calculation are 12.41 MeV, 9.1 fm and 3.90 MeV respectively. Subsequently, a coupled channels (CC) calculation for fusion was per-

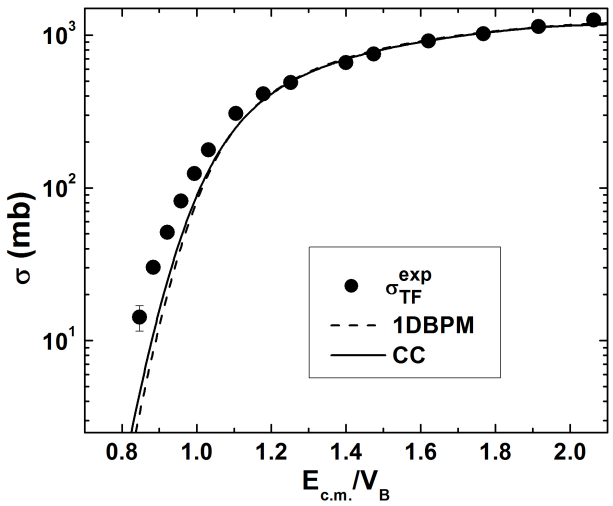

Figure 3. Experimental Fusion excitation function in comparison with model predictions of ^{6}Li+^{64}Ni. Dashed and solid lines represent the 1-DBPM and CC predictions respectively.

formed using the code CCFULL [18]. In the CC calculation both the projectile and the target excitations have been considered. The first excited state of ^{64}Ni (2^+, 1.345 MeV) and the first resonant state (3^+, 2.186 MeV) of the projectile ^{6}Li were coupled. The deformation parameters were taken from Refs. [19] for target and from [2] for the projectile. The breakup continuum of ^{6}Li or any other excited states of ^{64}Ni were not taken into consideration. The CC prediction has been shown in the Fig. 3 by solid line. The comparison of theoretical predictions and the data shows that both 1-DBPM and coupled channels calculations reproduce the above barrier fusion cross section values quite well. However, the experimental cross sections at the sub-barrier energies are significantly enhanced compared to the calculated values. The CC calculation marginally improves the description of the data at sub barrier region. To further explore the enhancement of fusion cross section below the barrier,we have plotted in Fig. 4 the enhancement factor EF defined as:

$$EF = \frac{\sigma_i}{\sigma_{1-DBPM}} \quad (1)$$

where i= TF or CC as a function of $E_{c.m.}/V_B$. It is observed from Fig. 4 that the both TF and CC predictions are nearly unity at above-barrier energies. As the energy decreases below the barrier both of them start to increase beyond unity. But the enhancement with respect to 1-DBPM rate is much higher for experimental TF than the CC prediction. It is to be noted that the estimated enhancement of CC prediction primarily indicates the possible enhancement of complete fusion cross sections due to coupling estimated from the code CCFULL. On the other hand, the enhancement observed for TF cross sections is probably due to the comparable contributions of incomplete fusion and/or the transfer processes at below barrier energies. Similar observation was also found in Ref.[20]. Identification of the reaction mechanisms contributing to

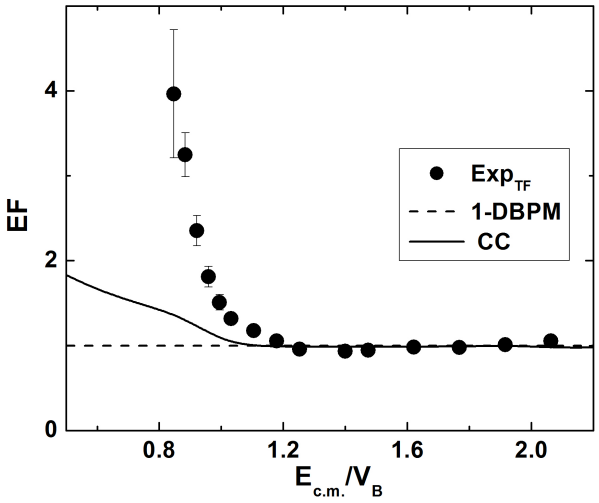

Figure 4. Enhancement factor (EF) as a function of the ratio of incident energy and the Coulomb barrier. Dashed and solid lines represent the 1-DBPM and CC predictions respectively. Details are given in the text.

the enhancement below the barrier is, therefore, of utmost importance.

4 Summary and Conclusion

The measurement of the TF excitation function has been performed for the reaction of stable weakly bound projectile ^{6}Li with the medium mass target ^{64}Ni at the near-barrier energies. The identification and cross section measurement of evaporation residues have been done using the prompt characteristic γ-ray detection technique. The measured σ_{TF} shows a good agreement with both the 1-DBPM and CC predictions in the above-barrier energies. So, there is no suppression of TF cross sections in this energy region. The observation is compatible with the earlier conclusion that TF is unaffected by the breakup of projectile irrespective of target mass [1–5, 7–10, 20]. But in the below-barrier region significant enhancement of total fusion cross sections is observed. This enhancement can not be explained by the coupling to the excited states of target and projectile. However, coupling to the continuum and coupling to one particle stripping channels leading to unbound ejectiles, have not been included in the calculation. It will be interesting to see the effect of these couplings on the total fusion at below-barrier energies. However, it is absolutely necessary to identify experimentally the reaction mechanisms contributing to the cross sections in order to understand the enhancement in this energy regime.

Acknowledgments

We sincerely thank the Pelletron staff for providing steady and uninterrupted ^{6}Li beam. We would also like to thank Mr. Aditya Agnihotri, Mr. Kiran Divekar and Prof. R. Palit of DNAP, TIFR and Dr. Rahul Tripathy, RCD, BARC for their support and cooperation during the experiment. The authors, Md. Moin Shaikh and S. Rajbanshi would like to thank the Council of Scientific & Industrial Research, India for financial support.

References

[1] M. Dasgupta *et al.*, Phys. Rev. C **70**, 024606 (2004).
[2] C. Beck *et al.*, Phys. Rev. C **67**, 054602 (2003).
[3] P.R.S. Gomes et al., Phys. Lett. B **601**, 20 (2004).
[4] A. Mukherjee*et al.*, Phys. Lett. B **636**, 91 (2006).
[5] P.R.S. Gomes *et al.*, Phys. Rev. C **71**, 034608 (2005).
[6] M. K. Pradhan *et al.*, Phys. Rev. C **83**, 064606 (2011)
[7] P.K. Rath *et al.*, Phys. Rev. C **79**, 051601(R) (2009).
[8] D.J. Hinde *et al.*, Phys. Rev. Lett. **89**, 272701 (2002).
[9] P.R.S. Gomes *et al.*, Phys. Rev. C **84**, 014615 (2011).
[10] H. Kumawat *et al.*, Phys. Rev. C **86**, 024607 (2012).
[11] M. Biswas *et al.*, Nucl. Phys. A **802**, 67 (2008).
[12] P.R.S. Gomes *et al.*, Nucl. Instrum. Meth. Phys. Res. A **280**, 395 (1989).
[13] Computer code LAMPS (Linux Advanced Multiparameter System), www.tifr.res.in/∼pell/lamps.html.
[14] R. Liguori Neto *et al.*, Nucl. Phys. A **512**, 333 (1990).
[15] S.B. Moraes *et al.*, Phys. Rev. C **61**, 064608 (2000).
[16] A. Gavron, Phys. Rev. C **21**, 230 (1980).
[17] O. Akyüz and A. Winther, *Proc. Int. School of Physics Enrico Fermi, course LXXVII*, ed. R. A. Broglia, R. A. Ricci and C. H. Dasso (Noah-Holland, Amsterdam, 1981) p. 492.
[18] K. Hagino, N. Rowley, A.T. Kruppa, Comput. Phys. Commun. **123**, 143 (1999).
[19] B. Pritychenko, J. Choquette, M. Horoi, B. Karamy, B. Singh, At. Data Nucl. Data Tables **98**, 798 (2012).
[20] A. Di Pietro *et al.*, Phys. Rev. C **87**, 064614 (2013).